Hydrodynamic theory for granular gases

Rosa Ramírez,[1,2,*] Dino Risso,[3,*] Rodrigo Soto,[2,*] and Patricio Cordero[1,*]
[1]*Departamento de Física, Universidad de Chile, Santiago, Chile*
[2]*CECAM, ENS-Lyon, 46 Allée d'Italie, 69007 Lyon, France*
[3]*Departamento de Física, Universidad del Bío-Bío, Concepción, Chile*
(Received 19 January 2000)

A granular gas subjected to a permanent injection of energy is described by means of hydrodynamic equations derived from a moment expansion method. The method uses as reference function not a Maxwellian distribution f_M but a distribution $f_0=\Phi f_M$, such that Φ adds a fourth cumulant κ to the velocity distribution. The formalism is applied to a stationary conductive case showing that the theory fits extraordinarily well the results coming from our Newtonian molecular dynamic simulations once we determine κ as a function of the inelasticity of the particle–particle collisions. The shape of κ is independent of the size N of the system.

PACS number(s): 81.05.Rm, 05.20.Dd, 51.10.+y, 47.70.Nd

I. INTRODUCTION

Granular systems subjected to a sufficiently strong excitation may have a fluidlike behavior [1,2]. From the very beginning several authors have attempted to derive hydrodynamic equations for these systems [3,4]. If the excitation of the granular system is through a permanent injection of energy, the fluid system may stabilize to a low density stationary gaseous state which necessarily is a nonequilibrium state and it usually is inhomogeneous as well. To develop the basic features of the theory of gaseous granular systems we restrict the analysis to the simplifying inelastic hard sphere model (IHS) [3].

Many authors studying granular gases have put particular attention to studying the spontaneous homogeneous cooling of a granular system using periodic boundary conditions [5,6]. This time dependent state is called *homogeneous cooling state* (HCS) and the understanding of its properties has been improving through many papers [7–10]. A crucial breakthrough was the realization by Goldshtein and Shapiro [7] that the homogeneous cooling distribution function has a scaling property with respect to the instantaneous temperature. Such distribution—which we will be calling f_{HCS}—is known in approximate forms [11,12]. It is known, among other things, that its fourth cumulant κ does not vanish and that it has a long velocity tail.

A nonequilibrium inhomogeneous gaseous system, on the other hand, is described by a distorted distribution function typically obtained from Boltzmann's equation expanding the distribution either in gradients of the hydrodynamic fields (Chapman–Enskog method) [13] or making a moment expansion (Grad method) [14]. For normal gases the expansion is made about the equilibrium Maxwell distribution.

In this paper we will assume that a low density nonequilibrium granular system has a local distribution function which can be obtained expanding about a distribution f_0 resembling f_{HCS} in the sense that it has a significantly nonvanishing fourth cumulant. We introduce a reference function [see Eq. (5) below] which is a Maxwellian distorted by a factor which incorporates the next nontrivial cumulant, a fourth cumulant, to the distribution function and then we undertake a perturbative *moment expansion* à la Grad about f_0 to solve Boltzmann's equation. Some authors have done some calculations in this direction but using the gradient expansion (Chapman–Enskog) method [15]. The point is that, without the notion of equilibrium, we expect that the reference state, f_0 in our case, should resemble more the homogeneous cooling state than the simple Maxwellian.

We study a two-dimensional system of hard disks, and the moment expansion—in dimension two—is an 8 moment expansion: the number density $n(\vec{r},t)$, the velocity field $\vec{v}(\vec{r},t)$, the granular temperature field $T(\vec{r},t)$, the pressure tensor $P_{ij}(\vec{r},t)$, and the heat flux vector field $\vec{Q}(\vec{r},t)$. The dynamic variables are not the components of the pressure tensor P itself but the components of the symmetric traceless part p_{ij} where $P_{ij}=p\,\delta_{ij}+p_{ij}$ and p is the hydrostatic pressure.

As it can be seen in Grad's paper [14] or in [16], the method yields *hydrodynamic equations* for all the fields mentioned above. In particular, the dynamic equations for p_{ij} and $\vec{Q}$ take the place of what would normally be the constitutive (transport) equations of standard hydrodynamics. This last point means that we are not assuming any constitutive equations whatsoever, their present counterparts are dynamic equations.

It is well established that, in the case of the IHS model for granular systems, Boltzmann's equation is modified in that the restitution coefficient r enters solely in the gain term of the collision integral and it does so in two forms. First the gain term has an overall factor r^{-2} and second, the distribution functions appearing in the gain term depend upon the precollision velocities, and these velocities depend on r [4].

When the modified Boltzmann's equation is used the stemming hydrodynamic equations get factors that depend on the *inelasticity coefficient* q,

$$q=\frac{1-r}{2} \tag{1}$$

($q=0$ in the perfectly elastic case) except that the mass con-

*URL: http://www.cec.uchile.cl/cinetica

tinuity equation and the momentum balance equation remain unchanged since mass and momentum continue being microscopically conserved.

In the context of Boltzmann's equation a dissipative gas satisfies the ideal gas equation of state

$$p = nT, \tag{2}$$

where the granular temperature T is defined in energy units as the average kinetic energy per particle. If we were to consider the Boltzmann–Enskog equation, then the inelasticity coefficient would enter through the Enskog collision factor χ, and the equation of state of a normal gas and a dissipative gas would differ, but in the present context Eq. (2) holds.

Usual moment expansion methods (as Grad's is) are appropriate to describe bulk properties. Wall effects are not well described unless higher order moments are included in the expansion, which are not trivial to handle [17]. Already in normal gases hydrodynamic fields may have discontinuities at walls. In a previous paper we gave a kinetic description of a one-dimensional granular system with theoretical tools such that our description was correct and precise up to the walls [18] but we have not generalized yet that type of formalism to higher dimensions, hence, in the present paper, we use moment expansions.

In consequence the formalism we are going to present suffers too of the weakness of moment expansions: it is unreliable precisely at the points where the boundary conditions should be imposed forcing us to trade the boundary conditions for conditions imposed far from the walls based on the actual behavior of the system according to our molecular dynamic simulations.

Our moment expansion method, explained in detail in Sec. II, uses as reference distribution function a distribution f_0 which differs from a Maxwellian distribution in that it has a nonvanishing fourth cumulant, κ. The method leads to hydrodynamic equations for low density granular systems that depend parametrically on the inelasticity coefficient q and κ. We apply these hydrodynamic equations to a stationary and purely conductive case as in [19]. The value of the fourth cumulant κ, or better, the dependence of the fourth cumulant on q is determined directly from molecular dynamic simulations, and it turns out to be independent of the size N of the system. The predictions that follow from our formalism agree very well with all our simulation data.

In Sec. II we briefly present the moment expansion method, in Sec. III the hydrodynamic equations that follow are given and specialized to a purely conductive case, and finally in Sec. IV theory and simulational results are compared. Final comments are in Sec. V.

II. THE MOMENT EXPANSION METHOD FOR GRANULAR SYSTEMS

Moment expansion methods can summarily be described as follows. Take a velocity distribution function $f_0(\vec{r},\vec{c},t)$ which is considered to be the *reference function* about which an expansion is going to be made. For normal gases the natural choice for f_0 is a local Maxwellian distribution f_M written in terms of the peculiar velocity $\vec{C}=\vec{c}-\vec{v}(\vec{r},t)$, where $\vec{v}(\vec{r},t)$ is the hydrodynamic velocity. Next a set of orthonormal polynomials on $\vec{C}$, $H_a(\vec{C})$, are built in the sense that $H_0=1$ and

$$\int H_a(\vec{C})H_b(\vec{C})f_0(\vec{r},\vec{C},t)d\vec{C}=\delta_{ab}. \tag{3}$$

The polynomials H_a are obtained simply by building a base of orthonormal polynomials starting from $H_0=1$ and from first degree upwards. We have built polynomials only on C_i, C_iC_j and C^2C_i as Grad did, namely, up to third order and not all of them. One could go on but so far this seems to be enough. When f_0 is a Maxwellian the H_a are Hermite polynomials but in general they are not but they are still obtained in a straightforward way.

Next a distribution function of the form

$$f(\vec{r},\vec{C},t)=\left(1+\sum_a H_a(\vec{C})R_a(\vec{r},t)\right)f_0(\vec{r},\vec{C},t) \tag{4}$$

is defined and first it is checked that $\int f\,d\vec{c}=n$. The R_a are determined by systematically requiring that the averages taken with the above distribution in the form $\langle A\rangle_f \equiv (1/n)\int Af\,d\vec{c}$ give the correct quantities, such as $\langle mnC_iC_i\rangle_f=P_{ij}$. The result of this exercise is that the R_a are simple combinations of the hydrodynamic fields (such as P_{ij}).

The following step is to replace the above distribution in Boltzmann's equation to derive integrability conditions multiplying the kinetic equation consecutively by the H_a and integrating the equation over $\vec{C}$. The idea is to do this up to a given order and drop all contributions coming from polynomials of degree higher than a chosen value (up to order 3 in our case). These integrability conditions turn out to be a set of hydrodynamic equations for the different moments.

A key point is the choice of the reference function f_0. The two-dimensional Maxwellian $f_M=n(m/2\pi T)\exp[-mC^2/(2T)]$ is privileged as the solution describing the equilibrium state of a normal gas. Since in granular systems there is no such thing as equilibrium a next best choice, seems a distorted Maxwellian distribution [11]

$$f_0=\left[1+\frac{\kappa}{2}\left(1-\mathcal{C}^2+\frac{\mathcal{C}^4}{8}\right)\right]f_M \tag{5}$$

where the dimensionless peculiar velocity is

$$\vec{\mathcal{C}}=\sqrt{\frac{m}{T}}\vec{C} \tag{6}$$

and T is the granular temperature. The coefficient κ is the fourth cumulant of f_0 and it depends on the inelasticity coefficient q while the coefficients in front of $\mathcal{C}^2$ and $\mathcal{C}^4$ are derived from requiring that f_0 is normalized and that $\langle (m/2)C^2\rangle_{f_0}=T$. The fourth cumulant κ in dimension two is

$$\kappa=\frac{\langle\mathcal{C}^4\rangle-2\langle\mathcal{C}^2\rangle^2}{\langle\mathcal{C}^2\rangle^2}, \tag{7}$$

In the case of the homogeneous cooling state, recent papers have justified explicit forms [11,12] for κ in the context of distribution functions like f_0. Their results are well approximated by

$$\kappa = \frac{b_1 + b_2 q}{1 + b_3 q} q, \tag{8}$$

with

$$b_1 = -2, \quad b_2 \approx 13.619, \quad b_3 \approx 4.5969. \tag{9}$$

The rational expression given in (8) is valid within 2.9% for $q \leqslant 0.08$, $r = 1 - 2q \geqslant 0.84$. Notice that $\kappa(q=0) = 0$ allowing to recover the elastic case.

We describe quite satisfactorily nonhomogeneous, nonequilibrium stationary states with a κ as in (8), but with numerical factors different from those in Eq. (9). The latter values are valid only for the homogeneous cooling state while our system is kept in a stationary inhomogeneous state with appropriate boundary conditions.

For any κ the distribution (4) with the explicit H_a obtained with the method summarized above is

$$f^{(\kappa)} = \left[1 + \frac{p_{xx}}{p(2+\kappa)} (\mathcal{C}_x^2 - \mathcal{C}_y^2) + 2 \frac{p_{xy}}{p(2+\kappa)} \mathcal{C}_x \mathcal{C}_y + \frac{Q_x}{2Q_0} \frac{(\mathcal{C}^2 - 4 - 2\kappa)\mathcal{C}_x}{(2 + 5\kappa - \kappa^2)} + \frac{Q_y}{2Q_0} \frac{(\mathcal{C}^2 - 4 - 2\kappa)\mathcal{C}_y}{(2 + 5\kappa - \kappa^2)} \right] f_0, \tag{10}$$

where we have used that $p_{yy} = -p_{xx}$ and $Q_0 = \sqrt{T/m}p$. The distribution $f^{(\kappa)}$ shares with f_0 the first scalar moments: density, temperature and fourth cumulant, for any value of q. If κ is chosen to be zero then, in Eq. (10), $f_0 \to f_M$ and $f^{(\kappa)}$ becomes the usual Grad's distribution. Hence the whole method would be the original method devised by Grad and, if κ is chosen to be Eq. (8) with coefficient values as in Eq. (9), then f_0 would be what we are calling f_{HCS}.

Given our ignorance regarding granular gases one could, in principle, accept f_M or f_{HCS} as legitimate reference functions to make the moment expansion. In the following sections we compare the three formalisms (reference functions f_M, f_{HCS}, and f_0, the latter with a κ adjusted to the results) concluding that only the one based on f_0 gives acceptable results for a sufficiently large range of q. In fact they are very good.

III. THE HYDRODYNAMIC EQUATIONS

As already mentioned, the inelasticity coefficient q enters the kinetic equation in two different forms. It appears as a factor $(1/r^2) = [1/(1-2q)^2]$ in the gain term and it appears in the expression for the precollision velocities which are part of the argument of the distribution functions appearing in the gain term. When the solution $f^{(\kappa)}$ is inserted in Boltzmann's equation, q enters in a still third form, precisely through the κ coefficient given by Eqs. (8) and (10). Expanding the collisional term of Boltzmann's equation in powers of q and κ, the moment method yields the following hydrodynamics equations for a granular gas.

First the mass and momentum balance equations get no contribution from the collisional term:

$$\frac{Dn}{Dt} + n \vec{\nabla} \cdot \vec{v} = 0 \tag{11}$$

$$m n \frac{D\vec{v}}{Dt} - n\vec{F} + \vec{\nabla} \cdot \mathsf{P} = \vec{0}. \tag{12}$$

But the balance associated to energy, to P_{ij} and to Q_k do get contributions from the collisional term,

$$n \frac{DT}{Dt} + \frac{\partial Q_k}{\partial x_l} + P_{lk} \frac{\partial v_k}{\partial x_l} = \frac{1}{2} \frac{\delta p}{\delta t}, \tag{13}$$

$$\frac{\partial P_{ij}}{\partial t} + \frac{\partial}{\partial x_l} (mn \langle C_i C_j C_l \rangle P_{ij} v_l) + P_{lj} \frac{\partial v_i}{\partial x_l} + P_{li} \frac{\partial v_j}{\partial x_l} = \frac{\delta P_{ij}}{\delta t}, \tag{14}$$

$$\frac{\partial Q_k}{\partial t} + \frac{\partial}{\partial x_l} \left(\frac{mn}{2} \langle C^2 C_k C_l \rangle + v_l Q_k \right) - \left[T \frac{\partial P_{ks}}{\partial x_s} + \frac{P_{sk}}{mn} \frac{\partial P_{sl}}{\partial x_l} + mn \langle C_l C_s C_k \rangle \frac{\partial v_s}{\partial x_l} + Q_l \frac{\partial v_k}{\partial x_l} \right] = \frac{\delta Q_k}{\delta t}, \tag{15}$$

where $\langle A \rangle$ refers to an average using $f^{(\kappa)}$ while $D/Dt \equiv \partial/\partial t + \vec{v} \cdot \vec{\nabla}$ and

$$\tau = \frac{1}{2\sigma p} \sqrt{\frac{mT}{\pi}} \tag{16}$$

is a characteristic relaxation time (σ is the diameter of the particles). The δ terms (colisional contributions) are

$$\frac{\delta p}{\delta t} = -\frac{2Ap}{\tau}, \tag{17}$$

$$\frac{\delta P_{ij}}{\delta t} = -\frac{B}{\tau} P_{ij} + \frac{B - 2A}{\tau} p \delta_{ij}, \tag{18}$$

$$\frac{\delta Q_k}{\delta t} = -\frac{C}{2\tau} Q_k. \tag{19}$$

The $\langle \cdots \rangle$ averages in Eqs. (12)–(15) and the coefficients A, B, and C when the generic distribution $f^{(\kappa)}$ is used turn out to be

$$mn \langle C_i C_j C_k \rangle = \tfrac{1}{2} (\delta_{ij} q_k + \delta_{jk} q_i + \delta_{ik} q_j), \tag{20}$$

$$mn \langle C^2 C_i C_j \rangle = \left(6 \frac{2 + 3\kappa}{2 + \kappa} P_{ij} - 2 \frac{2 + 5\kappa - \kappa^2}{2 + \kappa} p \delta_{ij} \right) \frac{T}{m}, \tag{21}$$

$$A(q) = [q(1-q) + O(q^5)] \left(1 + \frac{3}{32} \kappa + \frac{9}{4096} \kappa^2 \right),$$

$$B(q)=\frac{1+\frac{1}{2}q-\frac{3}{2}q^2+\frac{23}{32}\kappa\left(1+\frac{q}{2}\right)+\frac{\kappa^2}{4096}+O(q^3)+O(\kappa^3)}{\left(1+\frac{1}{2}\kappa\right)}, \tag{22}$$

$$C(q)=\frac{1+\frac{13}{2}q-\frac{15}{2}q^2+\frac{\kappa}{64}(206+1267q)-\frac{2415}{4096}\kappa^2+O(q^3)+O(\kappa^3)}{\left(1+\frac{5}{2}\kappa-\frac{\kappa^2}{2}\right)}.$$

They depend on q and κ, but κ depends on q. At least for small q the coefficients A, B, and C are positive (q varies between 0 and $\frac{1}{2}$). The coefficient A in Eq. (13) determines the energy dissipation in the system and consequently it vanishes in the elastic limit while B and C tend to 1.

It is our hope that the above hydrodynamics is valid in a wide variety of situations compatible with gaseous states and no clustering [5,8] but in this paper we restrict our study to a hydrostatic case.

We are going to consider the purely conductive regime, with no external force, $\vec{F}=0$. The system of N disks is in a rectangular box of dimension $L_x\times L_y$, with thermal walls, at $y=-\frac{1}{2}L_y$ and at $y=\frac{1}{2}L_y$, both at temperature T_0, and periodic boundary conditions in the X direction. The case with no external force is quite simple because the system is symmetric with respect to $y\to -y$ and the pressure turns out to be uniform. If the system were conservative, as a normal gas, this would be a homogeneous system at thermal equilibrium, but since the system is dissipative the temperature depends on the coordinate y (T has a minimum at the symmetry axis) and the problem is much less trivial. Since the system is purely conductive there is no velocity field, $P_{xy}=0$, $Q_x=0$ and the other fields depend only on the coordinate y.

More in detail, the mass continuity equation is an identity, the momentum balance equations imply that both P_{xy} and P_{yy} are uniform, the energy balance leads to $Q_y'=-2Ap/\tau$ (the prime denotes derivative with respect to y). The balance associated to the P_{ij} leads to $P_{xy}=0$ and to $Q_y'=-2Bp_{yy}/\tau$ which is a second expression for Q_y'. Combining both it follows that $p_{yy}=Ap/B$ hence both p_{yy} and p are uniform and

$$p=\frac{P_{yy}}{1+\frac{A}{B}}. \tag{23}$$

The balance associated to the Q_k says that

$$\left[\left(3\frac{2+3\kappa}{2+\kappa}\frac{AP_{yy}}{A+B}+2(2+\kappa)p\right)\left(\frac{T}{m}\right)\right]'=-CQ_y/(2\tau).$$

Combining all the previous results the set of equations (11)–(15) becomes

$$P_{xx}=\frac{B-A}{B}p,\quad P_{yy}=\frac{B+A}{B}p,$$

$$Q_y'=-4Ap^2\sigma\sqrt{\frac{\pi}{mT(y)}},\quad T'=-\frac{\sigma BC}{3A^*+2B^*}\sqrt{\frac{\pi m}{T}}Q_y, \tag{24}$$

with

$$A^*=\frac{2+3\kappa}{2+\kappa}A,\quad B^*=\frac{2+\kappa}{2}B, \tag{25}$$

where the prime indicates derivative with respect to y. Notice that because there is inelasticity the pressure tensor is anisotropic in the sense that $P_{xx}\neq P_{yy}$. In fact $P_{yy}-P_{xx}\sim A\sim q$ and they do not depend on the coordinate y.

Next we are going to compare the implications of these equations with our molecular dynamics results. To this end we should, in principle, solve these hydrodynamic equations using the boundary conditions associated to the particular simulations that we have studied. This is not a straightforward task because, as we have mentioned at the end of the introduction, the moment expansion method (behind the previous hydrodynamic equations) does not give a good description near boundaries. For example, if we impose that a wall behaves as a stochastic wall at temperature T_0, the observed field T is not expected to take that value near the wall. Later on it will be shown how we tackle this problem.

From Eq. (24) it is direct to derive that the temperature field satisfies the equation

$$TT''+\tfrac{1}{2}T'^2=k^2\sigma^2p^2, \tag{26}$$

where

$$k^2\equiv\frac{4\pi ABC}{3A^*+2B^*}. \tag{27}$$

Since the pressure is uniform, and because of Eq. (2), this equation can also be used as an equation for the inverse of the density.

Before proceeding to solve the equations we adimensionalize the problem defining a coordinate $\xi=y/L_y$, ($-\frac{1}{2}\leqslant\xi\leqslant\frac{1}{2}$) and we also define

$$\overline{n}=\frac{N}{L_xL_y},\quad n(y)=\overline{n}n^*(\xi),$$

$$K=\frac{k}{2\sqrt{2}}\left(\frac{N\sigma}{L_x}\right),\quad Q_y(y)=\overline{n}T_0\sqrt{\frac{T_0}{m}}Q_y^*(\xi),\qquad (28)$$

$$T(y)=T_0T^*(\xi),\quad p=\overline{n}T_0p^*.$$

Once Eq. (26) is solved and converted to a solution for the dimensionless number density $n^*(\xi)$ the result is

$$4K|\xi|=\frac{1}{n^*(\xi)}\sqrt{\frac{n^*_{\max}-n^*(\xi)}{n^*_{\max}}}+\frac{1}{n^*_{\max}}\operatorname{arctanh}\sqrt{\frac{n^*_{\max}-n^*(\xi)}{n^*_{\max}}},\qquad (29)$$

where $n^*_{\max}$ is the value taken by $n^*(\xi)$ in the middle of the system, $\xi=0$. In what follows it is shown that $n^*_{\max}$ is a simple function of the parameter K defined above. The effect of the boundaries is traded in favor of the observed values of $n^*_{\max}$.

The integral condition $\int n\,dx\,dy=N$ can be cast as

$$\int_0^{1/2} n^*d\xi=\tfrac{1}{2},\qquad (30)$$

but since $d\xi=(d\xi/dn^*)dn^*$ the integral condition yields,

$$\frac{n^*_b}{n^*_{\max}}=1-\tanh^2 K,\qquad (31)$$

where n^*_b is the value that $n^*(\xi)$ takes at the two boundaries, $n^*_b=n^*(\pm\frac{1}{2})$.

Equation (29) evaluated at $\xi=\frac{1}{2}$ yields a different condition over n^*_b and it follows that

$$n^*_{\max}=\frac{1}{2}+\frac{\sinh(2K)}{4K}.\qquad (32)$$

This is a strong result, it says that the dimensionless number density at the center, $n^*_{\max}$, is determined by K^2 alone,

$$K^2=a_0^2\frac{2ABC}{3A^*+2B^*},\qquad (33)$$

where $a_0^2=N\rho_A/\alpha$, $\alpha=L_x/L_y$ is the aspect ratio of the box, and $\rho_A=(\pi/4)(N\sigma^2/(L_xL_y))$ is the fraction of area occupied by the disks. Since A vanishes in the elastic limit and for small inelasticity coefficient q, $A\approx q$ while $B\approx 1$ and $C\approx 1$ then

$$K^2\approx a_0^2q\approx\frac{1}{\alpha}qN\rho_A.\qquad (34)$$

In the quasielastic limit then, the control parameter is basically $qN\rho_A$. This result, for fixed area density, resembles what we obtained in the one-dimensional case [18], namely, that the relevant control parameter of the one-dimensional equations is qN.

The temperature is $T^*(\xi)=p^*/n^*(\xi)$ but since the pressure is uniform one may be tempted to use $p^*=n^*_bT^*_b$ with the value for n^*_b already derived from the theory and the value T^*_b imposed in the simulation. This would give a bad fit however because, as we have been emphasizing, the formalism is not reliable near the boundaries. Therefore we choose for p^* the value $p^*=T^*_{\min}n^*_{\max}$. We know $n^*_{\max}$ from Eq. (32), and we take the value for $T^*_{\min}$ directly from our simulations. It may be said that $T^*_{\min}$ is a parameter to adjust our results.

The dimensionless heat flux becomes

$$Q_y^*(\xi)=\frac{3A^*+2B^*}{2BC}\frac{1}{a_0}\sqrt{\frac{p^*}{n^*(\xi)}}\frac{p^*}{n^*(\xi)^2}\frac{dn^*}{d\xi}.\qquad (35)$$

IV. SIMULATION-THEORY COMPARISON

In this section we compare the simulational results with the values given by three formalisms which use as reference function: (i) f_M, (ii) $f_{\rm HCS}$, and (iii) f_0. We are calling $f_{\rm HCS}$ the function like f_0 but with κ defined with the values given in Eq. (9). The molecular dynamic simulations are true Newtonian simulations in the sense that the history of each particle is integrated using standard collision rules. Our method has been described elsewhere [16,20,21].

Since the formalisms differ by terms of higher order in q their predictions are quite similar unless qN is large enough. Typically the Maxwellian theory and the one based on $f_{\rm HCS}$ are valid until about $qN=20$ and are reasonable until $qN=40$ while the theory based on f_0, with an adjusted κ, is valid for values of qN up to 200, and reasonably good until about $qN\approx 300$.

A. Simulational setup

We have performed simulations of a two-dimensional system of $N=2300$, $N=3600$, $N=10\,000$, and $N=19\,600$ inelastic hard disks inside a $L\times L$ box with lateral periodic boundary conditions while the upper and lower walls are kept at granular temperature $T_0=1$. The area fraction covered by the disks was chosen to be $\rho_A=0.01$ (in which case the nonideal corrections to the equation of state are less than 2%) while the qN dissipation parameter ranges from $qN=10$ up to $qN=400$. The observed hydrostatic pressure is in fact uniform within 1%, except very close to the walls, see Fig. 1. In the $N=2300$ case, the smallest simulated system, the ratio between the mean free path and the linear size of the system (Knudsen number) is 0.065 and it is smaller in the other cases. This value guarantees that not too close to the walls the fluid has a hydrodynamic behavior. The wall temperature T_0 is imposed sorting the velocity of the bouncing particles as if they were coming from a heat bath at $T=T_0$.

In every simulation the system was relaxed from an initial condition for a sufficiently long time. After the relaxation we measure local time averages of the main moments of the distribution (i.e., n, $\vec{v}$, T, P_{ij}, $\vec{Q}$) inside each one of a set of square cells. Taking advantage of the translation invariance in the X direction, it is natural to take horizontal averages getting, in this way, smooth vertical profiles for the observed hydrodynamic fields.

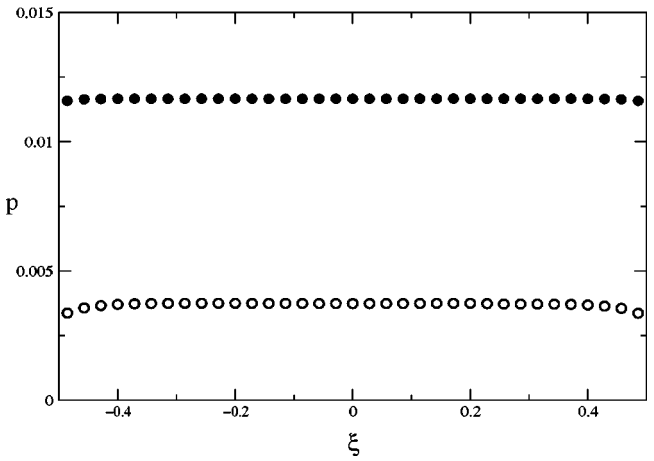

FIG. 1. The pressure profile in our simulations with $N=19\,600$, particles, area density $\rho_A=0.01$, and $qN=10$ (closed circles) and $qN=275$ (open circles). It can be appreciated that p is uniform except in a limited region near the walls where our formalism is known to fail.

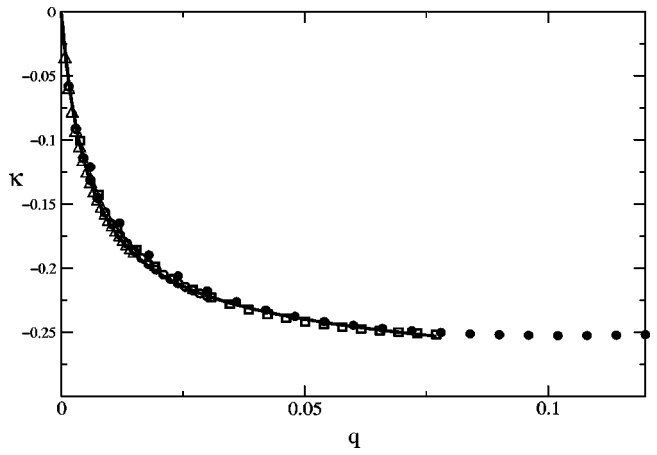

FIG. 2. The fourth cumulant κ against q for systems of different size. The empirical values of κ are represented by triangles for $N=19\,600$, empty circles for $N=10\,000$, empty squares for $N=3600$, and solid circles for $N=2300$. The solid line corresponds to our empirical fit. See text.

B. Theory and simulation comparison

In order to compare theory and simulation some analysis is needed because size effects are quite noticeable unless the number N of particles is above about 3600. We use expression (32) for $n^*_{\max}$ as our point of contact between theory and simulation and proceed to adjust the coefficients b_k in Eq. (8) so that K takes the values that makes theory give the observed values for $n^*_{\max}$.

With this aim we first write K as a rational expression $K=a_0\sqrt{q}(1+a_1q)/(1+a_2q)$ and find the values of the a_k so that Eq. (32) reproduces the observed values of $n^*_{\max}$. We have to adjust a_0 in spite of its definition, given under Eq. (33), because the effective values for the number of particles, the global density and the aspect ratio get distorted since there is a layer near the thermalizing walls which does not behave hydrodynamically. Once this expression for K is fixed, we invert (33) to obtain values for κ as a function of q. The size effect is in a_0 alone and $\kappa(q)$ is approximately the same for systems with N larger than about 3600, as shown in Fig. 2. In this figure there is a solid line which is Eq. (8) with

$$b_1=-44.77, \quad b_2=-27.96, \quad b_3=172.5. \tag{36}$$

The discrepancies between this curve and the empirical values of κ are less than 2% for the whole range of q considered. More in detail, Fig. 2 shows the behavior of $\kappa(q)$ for systems of different size. It is seen that in the case of $N=2300$ (solid circles) $\kappa(q)$ is dependent on the system's size, while the predictions in the cases $N=3600$, 10 000, and 19 600 differ among themselves by less than 2%. Only the smallest simulated system ($N=2300$) departs from this otherwise universal shape.

In the following we present the results corresponding to the $N=10\,000$ case.

(a) *The density*: As a first step and in order to check the validity of the kinetic description (no clustering, [5]) we have plotted the final configurational positions of the particles (not shown here) for different values of qN up to $qN=400$, finding that clustering begins at about $qN\approx300$. In fact, we have detected that the number of collisions per unit time increases dramatically shortly after $qN=300$.

As a second step we check the validity of Eq. (32) (which for fixed geometry depends only on qN) with simulations. The top of Fig. 3 shows both $n^*_{\max}$ (growing curves with qN) and n^*_b (the decreasing curves). It is seen how well the values of $n^*_{\max}$ (solid circles) come from the f_0 distribution (there should be no surprise as these are the fitted data), compared with the prediction using the other two distributions. This graph shows that $n^*_{\max}$ with the other two formalisms is good only up to $qN\approx40$.

Also at top Fig. 3 shows the values predicted by Eq. (31) and the observed values of n^*_b (see the caption), and it is seen that all theoretical schemes give values close to the simulational results in the considered range of qN. This is the only case where, for large qN, predictions coming from f_M are better that those coming from f_0, but we do not believe there is anything deep here since our moment expansion method is not reliable near walls.

Figure 3, bottom, compares theory and simulational density profiles for $qN=30$ and $qN=200$. As it has already been explained, the value $n^*_{\max}$ in Eq. (29) is fixed by Eq. (32) and there are no extra parameters to adjust. It is seen that theory in all cases (f_M, $f_{\rm HCS}$, and f_0) give good agreement for low values of qN. However predictions for $qN=200$, when using f_M or $f_{\rm HCS}$ fail. It is amazing how large qN can be when f_0 is used. In the last case the parameter K is adjusted only from the knowledge of $n^*_{\max}$ and it accurately predicts the behavior in almost all the volume. From the figure it can be appreciated that near the walls ($\xi=\pm0.5$), as mentioned in the introduction, the theory does not predict well the behavior of $n^*(\xi)$.

(b) *The temperature*: It has already been mentioned that the temperature profiles exhibit a minimum at the center and there is a temperature jump at the boundaries. In Fig. 4 we show the simulational results for $T^*_{\min}=T^*(\xi=0)$ and temperature $T^*_b=T^*(\xi=\pm1/2)$. It is seen that for $qN=40$ the temperature of the fluid by the walls is about 40% lower than the imposed value. This effect is due to dissipation and in 1D

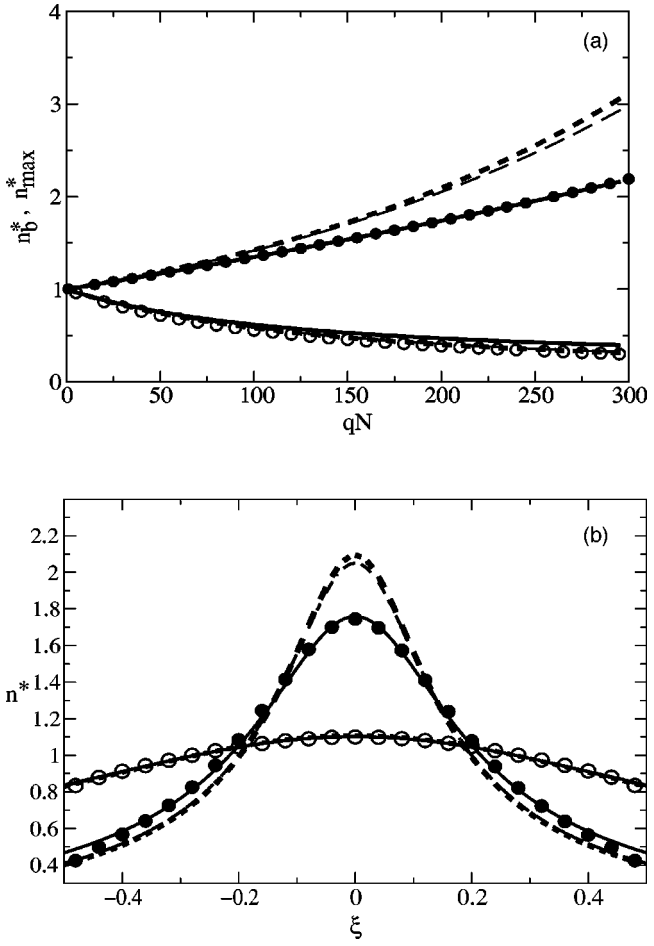

FIG. 3. At top the predicted and observed values for the density $n_{\max}^*$ at the center of the box ($\xi=0$) and n_b^* near the boundaries ($\xi=\pm 0.5$). The solid (open) circles correspond to the simulational values for $n_{\max}^*$ (n_b^*), the light-dashed (heavy-dashed) line corresponds to the theoretical prediction using f_{HCS} (f_M). The solid line corresponds to our empirical adjustment (see text). At bottom the predicted and observed density profiles for two different values of qN. The open (solid) circles correspond to $qN=30$($qN=200$). The light-dashed (heavy-dashed) line corresponds to the theoretical prediction using f_{HCS} (f_M). The solid line corresponds to the prediction stemming from f_0.

it has been shown to be a $O(qN)$ effect [18].

Because at present we have no theory to describe the temperature jump that takes place near the thermal walls, and we know that Grad's method does not give good results near boundaries, we have chosen the observed value of the temperature at mid height, $T_{\min}^*$, as the value to use in the formalism. The observed values decrease with qN and, in the case $N=10\,000$, we have adjusted them with the following expression:

$$\ln(T_{\min}) = -0.016\,3259qN + 5.276\,56\times10^{-5}(qN)^2 - 1.863\,96\times10^{-7}(qN)^3 + 4.241\times10^{-10}(qN)^4 - 4.238\,78\times10^{-13}(qN)^5 \quad (37)$$

whose faithfulness is shown in Fig. 4.

Since the pressure is uniform the temperature profile can be written directly as

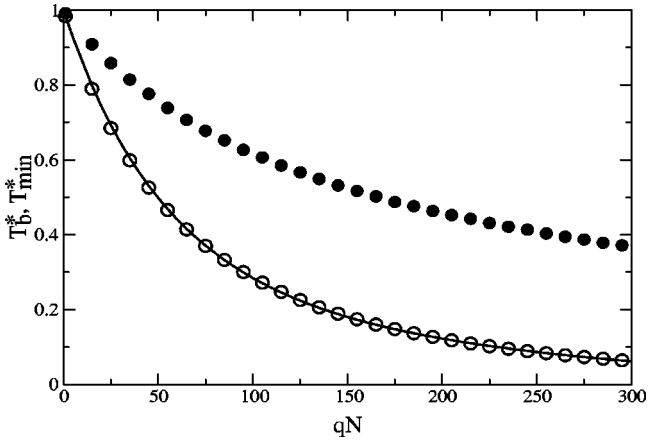

FIG. 4. Temperature $T_{\min}^*$ at the center of the channel (open circles) against dissipation qN. The solid line corresponds to a fit using Eq. (36). The solid circles are the observed values for the temperature T_b^* near the boundaries.

$$T^*(\xi) = \frac{T_{\min}^* n_{\max}^*}{n^*(\xi)}. \quad (38)$$

Figure 5 shows the simulational and theoretical temperature profiles for some values of qN. The three upper curves show the profiles for small qN values ($qN=10,20,30$) and it is seen that the predictions using f_0 (solid line) give an excellent fit to the simulational data while for the results obtained using f_M or f_{HCS} (dashed and light lines, respectively) the fit is only fair. The lowest curves shows T profiles for larger values of qN ($qN=50,100,200$). In this case only the formalism based on f_0 give an acceptable description and the agreement is very good up to $qN=200$. In the case of $qN=275$, not shown, there is still a reasonable agreement when f_0 is used.

(c) *The pressure*: Now that the values of $n_{\max}^*$ and $T_{\min}^*$ are known and since the pressure is uniform (both in theory and simulationally) and theory asserts that $p^*=T_{\min}^* n_{\max}^*$, then we have the value of p^*.

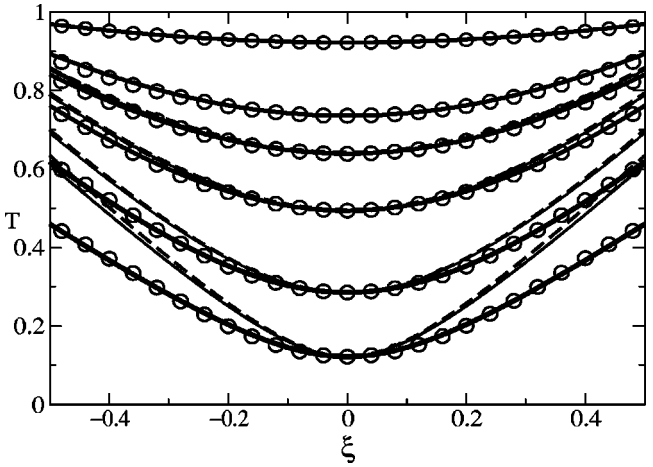

FIG. 5. From top to bottom temperature profiles corresponding to $qN=5,10,30,50,100$, and 200. The empty circles are the simulational results, the dashed line (light-solid line) correspond to the predictions obtained with f_M (f_{HCS}). The heavy-solid lines are the theoretical results when f_0 is used.

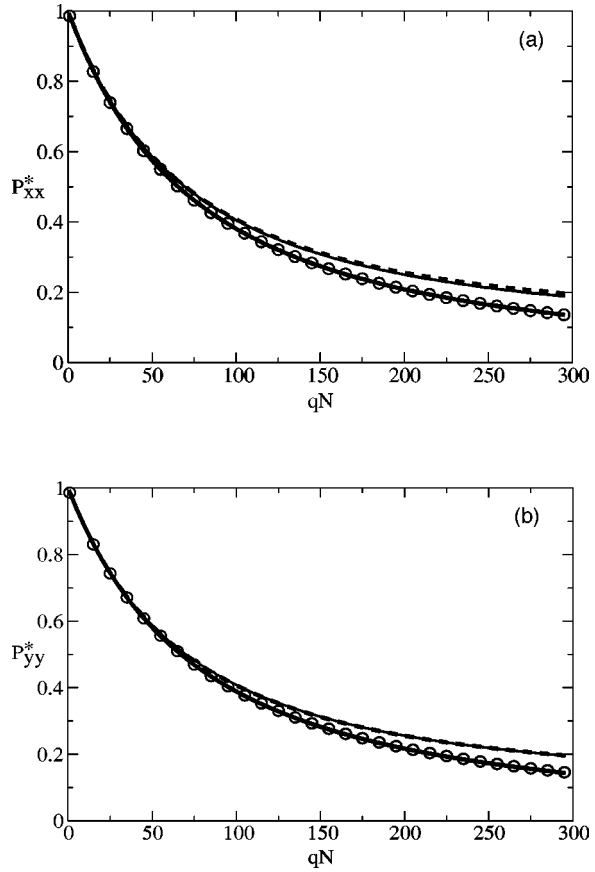

FIG. 6. Simulational and theoretical values for the components of the pressure tensor against dissipation qN. At top (bottom) the P_{xx} (P_{yy}) component. In light-solid line (dashed line) the theoretical results when using f_{HCS} distribution (f_M distribution). The heavy-solid line is the theoretical result when using the f_0 distribution.

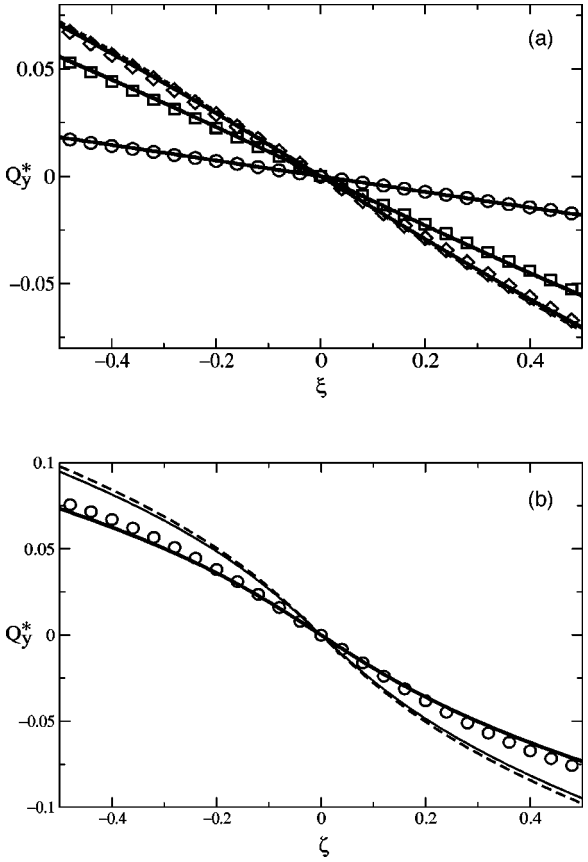

FIG. 7. Simulational and theoretical values for the heat flux profiles. At top the three curves and set of simulational data correspond to $qN=5$ (circles), $qN=20$ (squares), and $qN=30$ (rhombus). The dashed and light-solid lines correspond to the predictions using f_M and f_{HCS}, respectively, the heavy-solid line corresponds to f_0. At bottom are the observed values of Q_y^* when $qN=200$ and, the theoretical predictions when using f_0 (heavy-solid line), f_M (dashed line), and f_{HCS} (light-solid line).

From the value for the pressure and the set of Eqs. (24) one gets the theoretical values for P_{xx} and P_{yy} as a function of qN. These values are compared with our simulational data in Fig. 6. Again the comparison is good when the formalism with f_0 is used and it is only fairly good with the other two formalisms.

As it has already been mentioned after Eq. (24), the two diagonal terms of the pressure tensor are not equal because the system is anisotropic.

(d) *The heat current*: Equation (35) gives the theoretical expression for the heat current Q_y^*. The top of Fig. 7 shows simulational data and theoretical predictions for small values of qN. The three formalism predict well the observed values. The bottom of Fig. 7 it is possible to see that for $qN=200$ only the formalism using f_0 fits the observed data, while the other two fail badly. In the case of $qN=275$ the agreement is still reasonable within about 5%.

V. FINAL COMMENTS

In this paper we have studied a bi-dimensional granular system of N inelastic hard disks (normal restitution coefficient r). The system is placed in a rectangular box and it is kept in a stationary regime with upper and lower walls at granular temperature T_0. The lateral walls are periodic. Keeping the area density fixed to $\rho_A=0.01$ the quantity qN has been used as control parameter, where $q=(1-r)/2$, and simulations were made with different values of N ranging from $N=2300$ to 19 600. If the system were conservative it would remain in a perfectly homogeneous state at temperature T_0. Because there is dissipation the dimensionless number density n^* has a maximum in the middle, n^*_{max}, and the dimensionless temperature T^* has a minimum, T^*_{min}, also at the center of the system. The pressure is uniform and $p^*=n^*_{\mathrm{max}}T^*_{\mathrm{min}}$.

We have derived hydrodynamic equations using a moment expansion method. This method has the fourth cumulant, κ, of the velocity distribution as a parameter and three possible κ's were considered. These are $\kappa=0$ which implies that the reference distribution function is a Maxwellian, and two κ's of the form Eq. (8), one with parameters b_k as in Eq. (9) which corresponds to using f_{HCS} as the reference function and the other one using the values b_k, Eq. (36), numerically determined to ensure that the values of the density at the middle of the system come out correctly. The last case gives our reference function f_0. The empirical rational form of $\kappa=\kappa(q)$, Eq. (8), in the case of the successful distribution f_0 turns out to be independent of the size of the system. The

fourth cumulant κ of f_0 has been obtained to fit the results of a particular hydrodynamic regime and we expect that the theory with the approximate expression Eq. (8) for κ will have different values for the coefficients b_k when different regimes are studied. In this sense it should not be surprising that the coefficients b_k associated to κ successfully used to describe the homogeneous cooling state (HCS) differ from those used in the present paper. The HCS is an intrinsically time dependent state freely evolving while the system that we have described is time independent and it is continuously being excited by an energy injection. Furthermore, from the moment expansion viewpoint, κ is one additional moment and it should have been treated in the same footing as the other ones (n, v_i, T, P_{ij}, and Q_k), namely, it should be treated as an extra hydrodynamic field. It is possible to do so but it is difficult and it does not give room for κ to enter but only linearly in the distribution function, and not in the way it appears in Eq. (10). We hope to get deeper into this question in the near future. When this f_0 is used, the comparison between the predictions and simulation results for $n^*_{\max}$, p^*, P^*_{xx}, P^*_{yy} against dissipation, and the density, temperature, and heat flux profiles are very good.

The obvious conclusion is that the formalism based on f_0 gives an excellent description of the behavior of the system for values of qN up to 200 and it gives a reasonable description up to qN nearly 300 (slightly above $qN \sim 300$ clustering begins), while the other formalisms fail beyond about $qN = 40$. We would like to add that clustering in our system cannot be directly related to clustering in the homogeneous cooling state (HCS). For the HCS it has been established that shearing breaks the homogeneous cooling state when $qN\rho_A \geqslant \pi^2/4$, which, translated mechanically to our case ($\rho_A = 0.01$) implies $qN \geqslant 247$. The threshold for clustering, as far as we know, is not known in the HCS case [22]. In our system no shearing is observed and clustering occurs at a higher value of qN than the shearing threshold for the HCS case. This is possibly so because our system is permanently being excited by the thermalizing walls delaying, with respect to the freely evolving homogeneous system, the appearance of any (shearing or clustering) instability.

It may be interesting to compare our results with those in [19] where a kinetic model is presented and its consequences in a Navier–Stokes approximation are analyzed. In [19] the authors studied the system for a range of the control parameter $qN\rho_A$, defined in Eq. (34), similar to the range we have used. Both formalisms, the present one and that in [19] lead to a uniform pressure and our Newtonian simulation results, as seen in our Fig. 1, show in fact that the observed pressure for a system with $N = 19\,600$, $\rho_A = 0.01$ and $10 \leqslant qN \leqslant 275$ is uniform to within 1%. It must be kept in mind that $\rho_A = 0.01$ means that nonideal gas effects in the equation of state amount to about 2%. Another point of interesting comparison is the ratio P_{yy}/P_{xx} which, from Eq. (23), is readily seen in our case to be $P_{yy}/P_{xx} = (B+A)/(B-A) \approx 1 + 2q + O(q^2)$. In [19] P_{xx} is our P_{yy} and vice versa. In their expression (51) the same ratio corresponds approximately to $1 + 4q + O(q^2)$ while their data coming from their direct simulation Monte Carlo (DSMC) integration of Boltzmann's equation (see their Fig. 7) suggests that the actual ratio is much nearer to the $1 + 2q$ behavior obtained using Grad's method. The authors explain that this theory DSMC discrepancy has its origin in that the viscosity and conductivity coefficients cannot be adjusted simultaneously with the kinetic model and they chose to adjust the first.

In [15] the authors (Brey *et al.*) present hydrodynamic equations for the three-dimensional granular system derived using the Chapman–Enskog gradient expansion method [their Eqs. (56)–(58)]. One important difference is that the Chapman–Enskog method up to the order used by the authors leads to an isotropic pressure tensor while, as we have stressed before, Grad's method cannot escape having $P_{xx} \neq P_{yy}$. These authors make use of an interesting generalized Fourier's law with a term proportional to $\vec{\nabla} n$ besides the standard $\vec{\nabla} T$ term. On the other hand, as it is typical in Grad's method a dynamical equation for Q_k, Eq. (15), is obtained. It depends on the gradients of several fields and, in a generic stationary case, the implied transport law is highly nonlinear with, among others, terms containing $\vec{\nabla} n$. It would be difficult to attempt, in the length of a final comment, a thorough comparison between the two approaches. In the purely conductive case studied by us in the present paper a Fourier type of law is obtained with a conductivity which depends on q, κ, and T and this is compatible with the presence of a $\vec{\nabla} n$ term, as in [15], since both, for the Grad and the Chapman–Enskog method the pressure is uniform and $p = nT$, implying that $\vec{\nabla} n$ is proportional to $\vec{\nabla} T$ and then, once this term is absorbed in the traditional one, the effective thermal conductivity gets modified without any further consequences.

ACKNOWLEDGMENTS

This work has been partly financed by Fondecyt research Grant No. 296-0021 (R.R.), Fondecyt research Grant No. 1990148 (D.R.), Fondecyt research Grant No. 197-0786 (P.C.). One of us (R.S.) acknowledges a grant from MIDEPLAN and to FONDAP Grant No. 11980002.

[1] H.M. Jaeger and S.R. Nagel, Science **55**, 1523 (1992); H.M. Jaeger, S.R. Nagel, and R.P. Behringer, Phys. Today **49**, 32 (1996); Rev. Mod. Phys. **68**, 1259 (1996).

[2] J.A.C. Gallas, H.J. Herrmann, and S. Sokolowski, Physica A **189**, 437 (1992); Y. Zhang and C.S. Campbell, J. Fluid Mech. **237**, 541 (1992); S. Luding, H.J. Herrmann, and A. Blumen, Phys. Rev. E **50**, 3100 (1994); S. Warr, J.M. Huntley, and G.T.H. Jacques, *ibid.* **52**, 5583 (1995); N. Mujica and F. Melo, Phys. Rev. Lett. **80**, 5121 (1998).

[3] C.S. Campbell, Annu. Rev. Fluid Mech. **22**, 57 (1990).

[4] J.T. Jenkins and S.B. Savage, J. Fluid Mech. **30**, 187 (1983); C. Lun, S. Savage, D. Jeffrey, and R.P. Chepurnuy, *ibid.* **140**, 223 (1984); J.T. Jenkins and M.W. Richman, Arch. Ration. Mech. Anal. **87**, 355 (1985); Phys. Fluids **28**, 3485 (1985); P.K. Haff, J. Fluid Mech. **134**, 401 (1983).

[5] I. Goldhirsch, and G. Zanetti, Phys. Rev. Lett. **70**, 1619

(1993).
[6] S. McNamara, Phys. Fluids A **5**, 3056 (1993).
[7] A. Goldstein and M. Shapiro, J. Fluid Mech. **282**, 75 (1995).
[8] S. McNamara and W.R. Young, Phys. Rev. E **53**, 5089 (1996); R. Brito and M.H. Ernst, Europhys. Lett. **43**, 497 (1998); G. Peng and T. Ohta, Phys. Rev. E **58**, 4737 (1998); T.P.C. van Noije, M.H. Ernst, and R. Brito, *ibid.* **57**, R4891 (1998).
[9] J.J. Brey, F. Moreno, and J.W. Dufty, Phys. Rev. E **54**, 445 (1996); J.J. Brey, M.J. Ruiz-Montero, and D. Cubero, *ibid.* **54**, 3664 (1996).
[10] R. Soto, M. Mareschal, and D. Risso, Phys. Rev. Lett. **83**, 5003 (1999).
[11] T.P.C. van Noije Chn and M.H. Ernst, Granular Matter **1**, 57 (1998).
[12] N.V. Brilliantov and T. Pöschell, Phys. Rev. E **61**, 2809 (2000).
[13] J.H. Ferziger and H.G. Kaper, *Mathematical Theory of Transport Processes in Gases* (North-Holland, Amsterdam, 1972).
[14] H. Grad, in *Handbuch der Physik*, Vol. XII, edited by S. Füge (Springer, New York, 1958); in *Theory of Rarefied Gases in Rarefied Gas Dynamics*, edited by F. Devienne (Pergamon, New York, 1960).
[15] J.J. Brey, J.W. Dufty, C.S. Kim, and A. Santos, Phys. Rev. E **58**, 4638 (1998); V. Garzó and J.W. Dufty, *ibid.* **59**, 5895 (1999).
[16] D. Risso and P. Cordero, Phys. Rev. E **56**, 489 (1997); **57**, 7365(E) (1998).
[17] H. Struchtrup and W. Weiss, Phys. Rev. Lett. **80**, 5048 (1998).
[18] R. Ramírez and P. Cordero, Phys. Rev. E **59**, 656 (1999).
[19] J.J. Brey and D. Cubero, Phys. Rev. E **57**, 2019 (1998).
[20] M. Marin, D. Risso, and P. Cordero, J. Comput. Phys. **109**, 306 (1993).
[21] P. Cordero, and D. Risso, in *Fourth Granada Lectures in Computational Physics*, Vol. 493, edited by P.L. Garrido and J. Marro (Springer-Verlag, Berlin, 1997).
[22] J.T. Jenckins Richman, and M.W. Richman, Arch. Ration Mech. Anal. **87**, 355 (1985); R. Soto, M. Mareschal, and M. Malek Mansour, Phys. Rev. E (to be published).